Hindawi
Geofluids
Volume 2021, Article ID 8873542, 15 pages
https://doi.org/10.1155/2021/8873542

Research Article

Development of Modified Grouting Material and Its Application in Roadway Repair Engineering

Yang Yu[1], **Zhengyuan Qin**[2], **Xiangyu Wang**[3], **Lianying Zhang**[1], **Dingchao Chen**[1] and **Siyu Zhu**[1]

[1]*College of Civil Engineering, Xuzhou University of Technology, Xuzhou, Jiangsu 221111, China*
[2]*Nottingham Geospatial Institute, Jubilee Campus, University of Nottingham, Nottingham NG7 2TU, UK*
[3]*School of Mines, China University of Mining & Technology, Xuzhou, Jiangsu 221116, China*

Correspondence should be addressed to Zhengyuan Qin; originxzit@126.com

Received 30 July 2020; Revised 8 September 2020; Accepted 23 February 2021; Published 4 March 2021

Academic Editor: Qingdong Qu

It is very extraordinary for the success of coal mine roadway grouting with the following factors of high early strength, good fluidity, and convenient pumping, but the existing grouting materials make it difficult to achieve the above characteristics at the same time. Therefore, a modified grouting material is developed, which is composed of two kinds of dry materials A and B, which are mixed with water and in equal amounts. The physical and mechanical properties of modified grouting materials under different ratios were tested by laboratory orthogonal test, and the optimal ratio of grouting materials and additives was obtained: (1) the water-cement ratio is 0.8 : 1; (2) base material: the mass ratio of cement, fly ash, bentonite, and water is 1 : 0.3 : 0.1 : 1.44; (3) admixture: the mass ratio of water reducer C, accelerator D, and retarder E is 1.5% : 0.05% : 0.3%. The basic properties of the modified grouting materials were studied from the aspects of slurry flow state, diffusion range, and grouting parameters by using the numerical simulation method, and the reinforcement mechanism of slurry to the broken surrounding rock properties of the roadway was revealed: (1) the grouting pressure is the main factor affecting the slurry diffusion radius; (2) the mechanical properties of the roadway surrounding rock are improved, the plastic zone and deformation of surrounding rock are reduced, and the active support function of the anchor and cable is enhanced through grouting reinforcement; (3) the control effect of the roadway is improved, and the balanced bearing with anchorage structure of the roadway surrounding rock is realized through grouting reinforcement. On this basis, the modified grouting material is applied to roadway repair and reinforcement engineering practice. The field monitoring data show that the production practices were guided by roadway repair and reinforcement technology with the modified grouting material, as the core of the roadway surrounding rock control effect is good, and the modified grouting material has a wide range of application prospects.

1. Introduction

Coal is the main energy and important industrial raw material in China. With the increase of coal mining depth and intensity, there are a large number of complex and difficult roadways in the mine, including soft rock roadway, high stress roadway, strong dynamic pressure roadway, and broken surrounding rock roadway. Among them, the control of broken surrounding rock roadway has been one of the major problems perplexing coal mine safety production [1–6]. Under the influence of tectonic stress, mining stress, folding fault zone, and other factors, the surrounding rock of the roadway is seriously broken, the deformation is large, the failure rate of the support structure is high, and the control is difficult. According to statistics, 60%-80% of broken surrounding rock roadways need to be repaired many times to maintain their normal use, which leads to heavy maintenance workload, high cost, and poor safety [7–15].

In recent years, various grouting materials are used to reinforce the surrounding rock of roadway, fill cracks, cement broken surrounding rock, increase the integrity and

strength of surrounding rock, improve the self-supporting capacity of broken surrounding rock, improve the anchoring performance of supporting components, control the deformation of surrounding rock, and enhance the stability of roadway. The support and nursing concept and method are gradually applied to mine roadway repair engineering [16–20]. As the key and core factor, the comprehensive performance of grouting material will significantly affect the flow and diffusion range of slurry and ultimately determine the grouting reinforcement effect of the roadway. At present, many scholars have carried out effective research on grouting materials and developed grouting materials with different types and properties [21–34]. It can be divided into inorganic cement slurry and organic chemical slurry: (1) Inorganic cement slurry has the advantages of wide source, high strength of stone body, good impermeability, low price, convenient preparation, simple operation, nontoxic, and harmless. It is the most widely used and the largest amount of grouting material. However, it also has the disadvantages of large size, poor injectivity, long solidification time, and difficulty to control. In grouting engineering, cement admixture is usually added to the cement slurry to improve the water conductivity, stability, fluidity, and solidification properties of slurry, so that the slurry performance can meet the needs of field work. At present, cement slurry is developed in the direction of ultrafine cement, high water quick setting material, silica fume cement slurry material, and nanocement material. (2) Organic chemical grout has the advantages of low viscosity, good injectivity, strong impermeability, good solidification time control, good stability, small grouting pressure, and large slurry diffusion radius, but it also has the characteristics of high price, toxicity, fever, consolidation, low strength, strict construction technology requirements, and other defects and can easily cause coal washing difficulties, pollution of groundwater, and harm to human health, so its application scope is greatly limited.

At present, engineering materials research is focused on a wide range of sources, local conditions, environmental friendliness, and low price. In view of this, according to the characteristics of grouting reinforcement in broken surrounding rock stratum of roadway, a modified grouting material is developed by the author's team. Based on the different mineral composition and hydration mechanism of Portland cement and sulphoaluminate cement, full use was made of industrial solid waste fly ash to turn waste into treasure and reduce the cost of the modified grouting material, which not only has the advantages of adjustable solidification time and high strength, but also overcomes the shortcomings, such as easy pulverization, unstable chemical structure, and ease of corrosion by water. Through the experimental study, the best ratio of grouting materials under specific conditions is determined, and the flow diffusion laws and grouting reinforcement are revealed by numerical simulation. On this basis, the developed modified grouting material is applied to the repair project of broken surrounding rock roadway, which achieves the purpose of fast and stable solidification of broken coal and rock stratum and good control effect of roadway surrounding rock and effectively ensures the safe and efficient mining of coal resources.

2. Preparation of Modified Grouting Material

2.1. Determination of Composition

2.1.1. Grouting Mode. At present, the grouting mode is mainly divided into single liquid and double liquid. The single liquid is composed of one kind of slurry, the most common being cement slurry; the double liquid consists of two kinds of slurry, which are prepared and stored independently, and then injected into the matrix rapidly after the two are fully mixed. From the characteristics of mine roadway repair engineering, it is necessary to adjust the gelation time and early strength according to the broken degree of surrounding rock. Therefore, the modified grouting material adopts double liquid grouting mode.

2.1.2. Composition. The selection of grouting material composition is based on the wide sources of materials, low cost, strong comprehensive performance, and environmental friendliness. The grouting material is composed of two groups of dry materials A and B, which are mixed with water and in equal amounts. Material A is made of Portland cement, and material B is made of sulphoaluminate cement. Two kinds of dry materials with highly complementary chemical properties are composed of fly ash, bentonite, and additives. Before grouting, A material and B material are added into water, to make slurry. Both of them can maintain good fluidity within 2 hours. When grouting, the two slurries are fully mixed. By adjusting the proportion of the two materials, the condensation time can be achieved from a few minutes to several hours, and strength is produced by rapid hardening after condensation.

(1) *Cementitious materials*. The cementitious material of material A is Portland cement, which has the characteristics of stable strength development, high long-term strength, and large hydration heat due to its high content of silicate minerals. The cementing material of material B is sulphoaluminate cement, which has the characteristics of early strength, high strength, impermeability, and corrosion resistance. When the two kinds of cement are mixed in the proper proportion, the effect of quick setting and early strength can be achieved.

(2) *Active materials*. Fly ash is a kind of pozzolanic material with certain activity. It has fine particles, many spherical vitreous bodies, and smooth surface. It is distributed between cement particles and increases the compactness of the grouting body. Adding fly ash into cementitious materials can not only increase the fluidity of the paste but also recover industrial waste residue, reduce the amount of cement, and reduce the cost.

(3) *Bentonite*. Bentonite is a kind of clay mineral with montmorillonite as the main component. It has strong water absorption and is in suspension and gel state in aqueous solution. Using bentonite as the suspending agent can improve the dispersion and

suspension of solid particles of materials A and B in the slurry, avoid the phenomenon of sedimentation and bleeding, and make the material uniformly and stably hydrated to form a homogeneous hydration hardening body.

(4) *Admixtures*. It includes accelerator, water reducer in material A, and retarder and water reducer in material B. The main function of the admixture is to improve the pumping performance of material A and material B.

2.1.3. Mechanism of Hydration Reaction. The strength of double liquid grouting materials can be rapidly solidified, which is mainly due to the accelerated hydration reaction of Portland cement and sulphoaluminate cement. With Portland cement as the matrix and adding a certain amount of sulphoaluminate cement, the hydration of cement is promoted, the amount of ettringite in the hydration product increases, the setting time of composite cement is shortened, the early strength is increased, and the microexpansion is also observed. When sulphoaluminate cement is used as the matrix and a certain amount of Portland cement is added, the 24-hour strength of the composite system cement is increased, and the dry shrinkage rate of the cement is reduced. At the same time, the production cost of cement can be reduced without reducing the strength. Therefore, the addition of a small amount of other cement clinker has a great influence on the early hydration rate of the matrix cement, which is the same as the hydration mechanism of the matrix cement in the later stage, but it changes the relative proportion and microstructure of the hydration products of the system, thus improving its comprehensive performance.

2.2. The Optimum Ratio Test of Modified Grouting Material

2.2.1. Orthogonal Experimental Design. There are two characteristics of orthogonal experimental design method: balanced dispersion and uniformity. Compared with the uniform test method, the number of tests can be reduced regularly and only representative tests can be done. The correct estimation of test error and intuitive results can be obtained by range analysis. The orthogonal experiment design includes three aspects: (1) select factors and levels according to the experimental requirements, (2) select the orthogonal test table and develop a test plan according to the number of factors and levels, and (3) carry out experiments and analyze the test results.

In the design of slurry proportioning, the additive content is not considered at first, which involves three factors: water cement ratio, fly ash content, and bentonite content. The water cement ratio is the total mass ratio of water to cement, fly ash, and bentonite. The number of levels is determined according to the influence degree of each factor.

(1) Influence of Water-Cement Ratio on Compressive Strength of Slurry Stone. According to the previous test results [35–38], the setting time of Portland cement and sulphoaluminate cement is the shortest after mixing with the same amount. To make the slurry achieve the performance of rapid setting and early strength, the two are mixed according to the volume ratio of 1 : 1. The uniaxial compressive strength of mixed slurry stone under five different water-cement ratios is shown in Figure 1.

It can be seen from Figure 1 that with the increase of the water-cement ratio, the compressive strength of the slurry stone specimen gradually decreases, and the reduction range is obvious. When the water-cement ratio is 0.5 : 1, the compressive strength of the specimen is the highest, which reaches 5.6 MPa in 2 h and 22.8 MPa in 28 d; when the water-cement ratio is 1.5 : 1, the 28 d compressive strength of the specimen is 10.4 MPa, which is 12.4 MPa lower than that of the water cement ratio of 0.5 : 1; when the water cement ratio is 2.0 : 1, its compressive strength is the lowest, which is only 3.4 MPa at 28 d, which is 19.4 MPa lower than that of the 0.5 : 1 water cement ratio. Therefore, when the water-cement ratio is greater than 1.5 : 1, the strength of the slurry stone decreases significantly, which cannot meet the requirements of roadway engineering. Therefore, the water-cement ratio should not be greater than 1.5 : 1.

(2) Influence of Fly Ash on Compressive Strength of Slurry Stone. When the water-cement ratio is 1.0 : 1, the compressive strength of the slurry stone with different fly ash content is shown in Figure 2. It can be seen from Figure 2 that the cement concentration in the solution decreases because of addition of fly ash, the effective water-cement ratio for controlling the hydration rate of cement increases, and the calcium ion concentration decreases, which weakens the connection between particles and reduces the early compressive strength of the slurry stone.

With the increase of fly ash content, the latter strength of the slurry stone increases first and then decreases. When the content of fly ash is 20%, the compressive strength reaches the maximum, and the 28 d strength reaches 17.68 MPa, which is 16.32% higher than that of the specimen without fly ash. It is mainly due to the remarkable pozzolanic property of fly ash in the later hardening stage. When the content of fly ash is more than 30%, the strength at 2 h is 0 MPa and the strength at 28 d is only 14.8 MPa, which is lower than that of the specimen without fly ash. Therefore, the content of fly ash must be controlled in a certain range, preferably not more than 30%.

(3) Influence of Bentonite on Compressive Strength of Slurry Stone. When materials A and B are mixed with water to form slurry, the phenomenon of water separation will occur, which will affect the performance of the slurry. The addition of bentonite can improve the performance of slurry. When the bentonite is added into the slurry, the smaller montmorillonite particles will be attached to the surface of the larger cement particles due to the larger cement particles and the positive charge on the surface of the cement particles. Due to the good water retention, lubrication, and fluidity of the bentonite slurry, the cement particles will be suspended in the farther and finer rock cracks, thus preventing the cement slurry from solidification due to premature water loss. When the water-

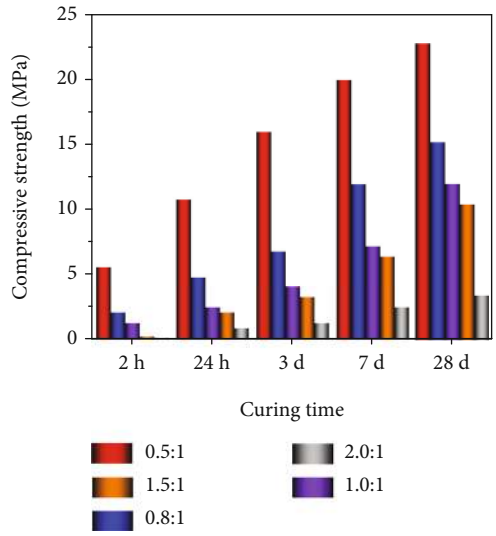

Figure 1: Relationship between water-cement ratio and compressive strength of slurry stone.

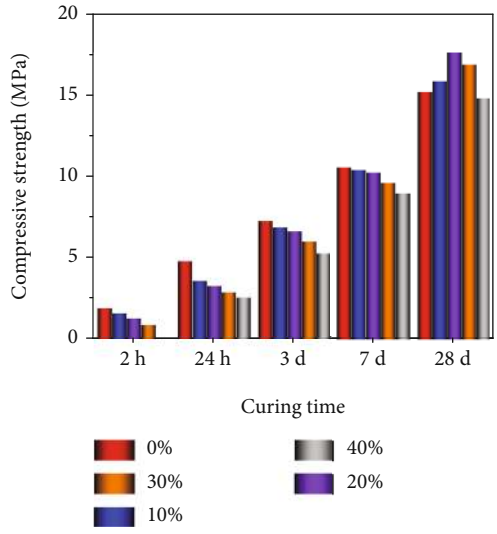

Figure 2: Relationship between slurry stone compressive strength and fly ash content.

cement ratio is 1.0 : 1, the water separation rate of single slurry A and B under different bentonite contents is shown in Figure 3(a). It can be seen from Figure 3(a) that with the increase of bentonite content, the slurry water separation rate gradually decreases. When the bentonite content exceeds 10%, the slurry suspension effect is better, and the water separation rate meets the general requirements. When the bentonite content is 20%, the slurry suspension effect is the best, the water separation rate of liquid A is 4.1%, and that of liquid B is 0%. Therefore, the bentonite content should be more than 10%.

When the water-cement ratio is 1.0 : 1, the compressive strength of bentonite slurry stone with different content is shown in Figure 3(b). It can be seen from Figure 3(b) that with the increase of bentonite content, the compressive strength of slurry stone gradually decreases, which is due to the fact that bentonite has almost no cementitious property. When the bentonite content is less than 15%, with the increase of bentonite content, the slurry stone strength decreases slightly, but the strength increases in 2 h. This is because a small amount of bentonite provides an alkaline environment, which speeds up the reaction time and shortens the condensation time.

In conclusion, three factors were selected in the orthogonal test, and three levels were selected for each factor. The levels and factors of orthogonal test are shown in Table 1. Using the L_9 (3^4) orthogonal test table, only 9 tests are needed.

The materials A and B are prepared into slurry. Firstly, Portland cement, sulphoaluminate cement, and fly ash are ground, and the fineness is controlled at the specific surface area of 400 m^3/kg. Then, the ground materials are mixed with water for 10 min according to the scheme. Finally, A and B solutions are mixed according to the volume ratio of 1 : 1. The ratio of the orthogonal test is shown in Table 2.

2.2.2. Comprehensive Performance Test Results and Mix Proportion Optimization

(1) Analysis of Physical Property Test Results. The test results of physical properties of A and B slurry are shown in Table 3.

According to the above test results, the range analysis method is used to determine the primary and secondary factors and determine the optimal level and combination. The range analysis method is simple and intuitive. The range analysis results of slurry viscosity, water separation rate, and condensation time are shown in Table 4.

According to the analysis results of slurry viscosity range, the water-cement ratio is the most important factor affecting the slurry viscosity, followed by the bentonite content, and finally the fly ash content. The optimal combination is $A_3C_1B_1$. The slurry viscosity decreases with the increase of water-cement ratio and increases with the increase of bentonite and fly ash content.

According to the range of analysis results of slurry water separation rate, the water-cement ratio is the most important factor affecting the water separation rate of single slurry A and B, followed by the content of bentonite, and finally the content of fly ash. The optimal combination is $A_1C_3B_1$. The increase of fly ash content will lead to the increase of water separation rate, while the increase of bentonite content will lead to smaller water separation rate and better slurry stability.

According to the range of analysis results of condensation time of slurry, the degree of importance of the impact on the condensation time, from large to small, is the water-cement ratio, bentonite content, and fly ash content. For comprehensive initial condensation and final condensation time, the optimal combination is $A_1B_1C_1$. The condensation time of slurry increases with the increase of the water-cement ratio, fly ash, and bentonite content, which is due to the decrease of cement relative concentration in slurry,

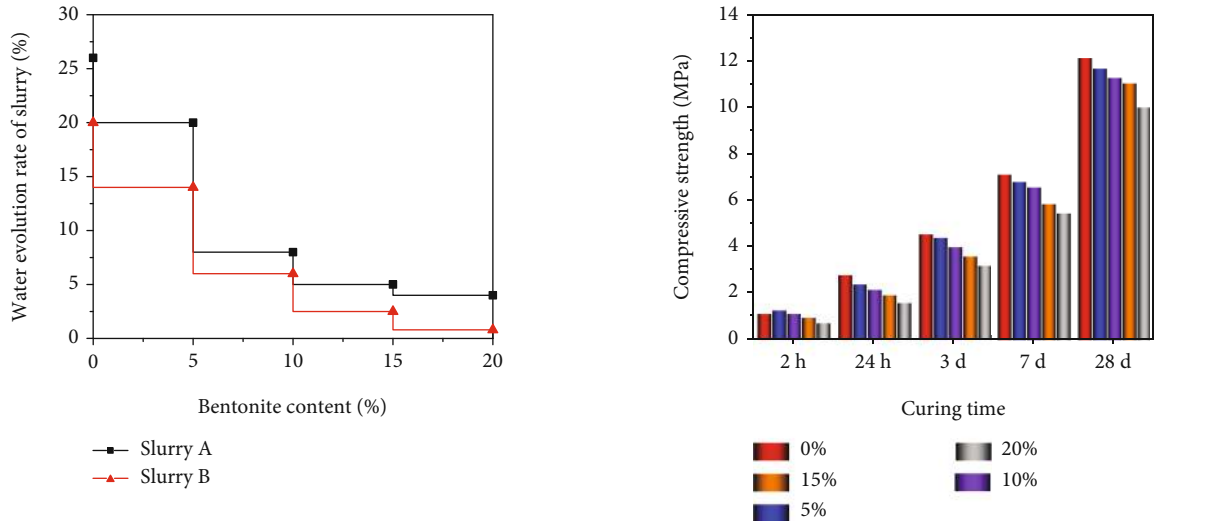

(a) Relationship between bentonite content and water separation rate (b) Relationship between bentonite content and compressive strength of slurry

Figure 3: Influence of bentonite on compressive strength of slurry.

Table 1: Factor level table of orthogonal test.

Level	Water cement ratio A	Mass percentage of fly ash B	Mass percent of bentonite C
1	0.5 : 1	10%	10%
2	0.8 : 1	20%	15%
3	1.0 : 1	30%	20%

Table 2: Orthogonal test group distribution ratio table.

Test serial number	Water cement ratio	Mass ratio of various materials		
		Cement	Fly ash	Bentonite
1	0.5 : 1	1	0.10	0.10
2	0.5 : 1	1	0.20	0.15
3	0.5 : 1	1	0.30	0.20
4	0.8 : 1	1	0.10	0.15
5	0.8 : 1	1	0.20	0.20
6	0.8 : 1	1	0.30	0.10
7	1.0 : 1	1	0.10	0.20
8	1.0 : 1	1	0.20	0.10
9	1.0 : 1	1	0.30	0.15

resulting in slower hydration rate and longer condensation time.

It can be seen that the water-cement ratio is the most important factor affecting the physical properties of the slurry. When the water-cement ratio is 0.8 : 1, the physical properties of the slurry are the best. Under the condition of this ratio, the stability and fluidity of the slurry are good, the stone rate is 100%, and the condensation time is moderate; the slurry with the water-cement ratio of 1.0 : 1 has a slightly poor stability and a slightly longer condensation time. Although the slurry with the water-cement ratio of 0.5 : 1 has good stability, it has a high viscosity and can only be used in special projects.

(2) Analysis of Mechanical Property Test Results. The test results of mechanical properties of slurry stone are shown in Table 5.

It can be seen from Table 5 that when the water-cement ratio is 0.5 : 1, the compressive strength of the slurry stone specimen is the highest, among which the mechanical properties of the first group of specimens are the best, the 2 h compressive strength is 5.09 MPa, and the 28 d compressive strength is 19.95 MPa; when the water cement ratio is 0.8 : 1, the mechanical properties of the sixth group of specimens are better, and the 28 d compressive strength is 15.48 MPa; when the water cement ratio is 1.0 : 1, the mechanical properties of the eighth group of specimens are better, and the 28 d compressive strength reaches 11.43 MPa.

According to the above test results, the range analysis method is used to determine the primary and secondary factors and determine the optimal level and combination. The range analysis method is simple and intuitive, and the range analysis results of compressive strength of slurry stone at different curing time are shown in Table 6.

The range analysis results show that the water-cement ratio has the greatest influence on the strength of the slurry stone, followed by the content of bentonite and fly ash. According to the requirements of general roadway grouting engineering, the early and late compressive strengths of materials are mainly investigated. The optimal combination of 2 h compressive strength is $A_1B_1C_1$, and that of 28 d compressive strength is $A_1C_1B_3$.

To sum up, when the water-cement ratio is 0.8 : 1, the physical properties of the slurry are the best, and when the water-cement solid ratio is 0.5 : 1, the mechanical properties

Table 3: Physical property test results.

Test serial number	Viscosity (s)	Water separation rate (%)		Coagulation (min)	
		Material A	Material B	Primary solidification	Final solidification
1	70.2	1.5	0.2	10	16
2	77.8	2.0	1.4	15	20
3	85.4	2.3	1.8	18	24
4	34.6	7.5	5.8	24	30
5	38.9	4.3	2.4	28	45
6	36.4	8.4	7.5	26	40
7	24.6	12.8	9.6	51	80
8	21.9	15.6	12.6	44	65
9	25.6	12.1	8.3	60	92

Table 4: Range analysis table of slurry physical performance.

Test items		Mean and range			Primary and secondary factors	Optimal combination
		A	B	C		
Viscosity	K_1	77.8	43.133	42.833	ACB	$A_3C_1B_1$
	K_2	36.633	46.2	46.267		
	K_3	24.033	49.133	47.3		
	R	53.767	6	6.8		
Water separation rate of material A	K_1	1.933	7.267	8.5	ACB	$A_1C_3B_1$
	K_2	6.733	7.3	7.2		
	K_3	13.5	7.6	6.467		
	R	11.567	0.333	2.033		
Water separation rate of material B	K_1	1.133	5.2	6.767	ACB	$A_1C_3B_1$
	K_2	5.233	5.467	5.167		
	K_3	10.167	5.867	4.6		
	R	9.034	0.667	2.167		
Primary solidification time	K_1	14.333	28.333	26.667	ABC	$A_1B_1C_1$
	K_2	26	29	33		
	K_3	51.667	34.667	32.33		
	R	37.334	6.334	6.333		
Final solidification time	K_1	20	42	40.333	ABC	$A_1B_1C_1$
	K_2	38.333	43.333	47.333		
	K_3	79	52	49.667		
	R	59	10	9.334		

of the slurry stone are the best, but the slurry viscosity under this ratio is large, the flow performance is poor, and it is difficult to pump. When the water-cement ratio is 0.8 : 1, the mechanical properties of the slurry stone can meet the engineering requirements. Therefore, considering that increasing the content of fly ash can effectively reduce the cost of slurry, the sixth group, namely, the mass ratio of cement, fly ash, bentonite, and water, is 1 : 0.3 : 0.1 : 1.44 as the optimal proportion of slurry.

2.3. Experimental Study on Slurry Admixture Ratio. The main performance requirements of modified grouting materials in mine roadway engineering include high early strength, good fluidity, and convenient pumping. The specific performance indexes of the modified grouting material are as follows.

(1) The condensation speed is fast and the early strength is high. The compressive strength is more than 2.0 MPa and not less than 15.0 MPa after 28 days

(2) The initial viscosity of the slurry is low, the fluidity is good, the slurry does not solidify within 2 hours, and the water separation rate is less than 5%

Table 5: Mechanical property test results.

Test serial number	Compressive strength (MPa)			
	2 h	24 h	3 d	28 d
1	5.09	10.03	14.11	19.95
2	3.11	6.94	11.32	18.77
3	1.66	5.02	8.28	17.25
4	1.31	4.01	6.05	13.01
5	0.82	2.99	5.10	11.09
6	1.05	3.43	5.88	15.48
7	0.49	2.41	4.12	9.51
8	0.59	3.01	5.03	11.43
9	0.3	1.88	3.92	10.98

(3) The gel time can be adjusted from a few seconds to a few minutes

However, reasonable admixtures should be added in practical application to make its strength performance and working performance meet the engineering requirements. In this experiment, the sixth group of slurry with a water-cement ratio of 0.8 : 1 was selected. The orthogonal test design method was used to study the influence of the content of water reducer C, accelerator D, and retarder E on the compressive strength of slurry stone. The content of admixture was comprehensively determined by measuring the compressive strength of slurry stone at 2 h, 24 h, 2 d, and 7 d. The test process and method are similar to the above optimized proportion of the slurry, so we will not repeat it. We only state the test results: the content of water reducer C and accelerator D has the greatest impact on the 2 d and 7 d compressive strength of the slurry, and the content of retarder E has a greater impact on the 2 h compressive strength of the slurry. From the point of view of improving the compressive strength of the slurry stone, the optimal ratio of the admixture content is finally selected. The mass ratio of water reducer C : accelerator D : retarder E is 1.5% : 0.05% : 0.3%.

3. The Action Mechanism of Slurry on Broken Rock Mass

3.1. Numerical Simulation Model. The process of grouting reinforcement of roadway surrounding rock involves two physical field coupling problems: stress field and seepage field. Therefore, the fluid analysis module in UDEC numerical simulation software is selected to establish fluid-solid coupling model by setting Bingham fluid model to simulate of slurry flow along surrounding rock fracture of roadway. Taking the belt transportation roadway of Qipanjing coal mine in Inner Mongolia of China as the research background, a numerical calculation model is established. Considering the boundary conditions of roadway and grouting, leakage, and other factors, the size of the model is length × height = 100 m × 83.2 m. The upper boundary of the model is a stress boundary. The vertical load is about 11.3 MPa calculated by the buried depth of 450 m. The length × height of the roadway is 5.2 m × 3.6 m. The grouting slurry is designed as cement slurry with the following main parameters: density 1500 kg/m^3, viscosity 25 Pa·s, and yield strength 5.0 MPa. The grouting hole is located at the end of the bolt. The designed grouting depth is 3.0 m, and the sealing length is 1.0 m. The grouting reinforcement is carried out after the roadway excavation and the implementation of bolt support. The constitutive model is the Mohr-Coulomb model. The mechanical parameters of the rock stratum and structural plane are shown in Tables 7 and 8.

3.2. Influence of Grouting Parameters on Grout Diffusion Range. By changing the two key parameters of grouting pressure and water-cement ratio, the variation law of slurry diffusion range is studied. The statistical results are shown in Figure 4. It can be seen from Figure 4 that when the distribution of surrounding rock fissures is fixed, the grouting pressure has a greater influence on the slurry diffusion range, while the water-cement ratio has a small impact. However, with the increase of grouting pressure, the influence of grouting pressure on the diffusion range of slurry decreases, and the influence of the water-cement ratio gradually increases. Therefore, the grouting pressure should not exceed 2.0 MPa, the water cement ratio is about 0.8 : 1, and the slurry diffusion range can meet the requirements of general roadway engineering.

3.3. Distribution of Grouting Pressure in Surrounding Rock. When the water-cement ratio of slurry is 0.6 and 0.8, respectively, the distribution curve of slurry pressure along the axial direction of grouting hole is shown in Figure 5 under different grouting pressure conditions. It can be seen from Figure 5 that the slurry pressure reaches the peak value about 1.2 m away from the roadway surface, the slurry pressure diffuses to the roadway surface for a short distance, the pressure attenuation is fast, and the attenuation is 0 MPa when reaching the roadway surface; the slurry pressure diffuses to the deep part of the surrounding rock of the roadway, the attenuation speed is slow, and there is still a certain residual pressure after attenuation of 3.0 m. Therefore, while increasing the grouting pressure to increase the spreading range of the grout, it is necessary to seal the surface of the roadway. In addition, the grouting pressure distribution curve is similar under different grouting pressure conditions. With the decrease of water-cement ratio, the grouting pressure decreases continuously.

3.4. Influence of Grouting on Plastic Zone of Surrounding Rock of Roadway. Two kinds of working conditions of repairing and strengthening the deformed and damaged roadway are simulated, respectively: (1) bolt and cable support alone and (2) grouting in the roadway first and then supporting with bolt and cable. The distribution characteristics of the plastic zone of surrounding rock under two working conditions are shown in Figure 6. It can be seen from Figure 6 that the plastic zone of the roadway with bolt and cable support based on grouting is smaller than that of simple bolt and cable support, especially on the two sides of roadway with an average reduction of more than 40%. It shows that grouting reinforcement technology in broken surrounding rock can improve the mechanical properties of surrounding rock,

Table 6: Range analysis table of mechanical properties of slurry stone.

Test items		Mean and range A	B	C	Primary and secondary factors	Optimal combination
Compressive strength of 1 h	K_1	3.287	2.297	2.243	ABC	$A_1B_1C_1$
	K_2	1.060	1.507	1.573		
	K_3	0.460	1.003	0.990		
	R	2.827	1.294	1.253		
Compressive strength of 24 h	K_1	7.330	5.483	5.490	ABC	$A_1B_1C_1$
	K_2	3.477	4.313	4.277		
	K_3	2.433	3.443	3.473		
	R	4.897	2.040	2.017		
Compressive strength of 3 d	K_1	11.237	8.093	8.340	ACB	$A_1C_1B_1$
	K_2	5.677	7.150	7.097		
	K_3	4.357	6.027	5.833		
	R	6.880	2.066	2.507		
Compressive strength of 28 d	K_1	18.675	14.157	15.620	ACB	$A_1C_1B_3$
	K_2	13.193	13.763	14.253		
	K_3	10.640	14.570	12.617		
	R	8.017	0.807	3.003		

Table 7: Rock mechanics parameters.

Rock stratum	Bulk modulus (GPa)	Shear modulus (GPa)	Internal friction angle (°)	Cohesion (MPa)	Tensile strength (MPa)
Overlying strata	9.80	8.00	34	5.50	2.10
Main roof	6.40	5.30	28	3.30	1.90
Immediate roof	4.50	4.90	27	3.10	1.70
9# coal seam	2.60	2.50	20	1.20	1.30
Immediate floor	4.80	4.80	28	2.90	1.68
Main floor	5.40	5.30	28	3.35	1.89
Underlying strata	9.70	8.32	33	5.40	2.06

Table 8: Mechanical parameters of contact surface.

Rock stratum	Normal stiffness (GPa)	Tangential stiffness (GPa)	Internal friction angle (°)	Cohesion (MPa)	Tensile strength (MPa)
Overlying strata	4.90	0.45	30	0.27	0.11
Main roof	3.20	0.26	24	0.16	0.08
Immediate roof	2.92	0.18	19	0.11	0.05
9# coal seam	1.11	0.10	16	0.06	0.03
Immediate floor	2.82	0.16	18	0.12	0.06
Main floor	3.31	0.24	23	0.15	0.09
Underlying strata	4.86	0.46	32	0.26	0.12

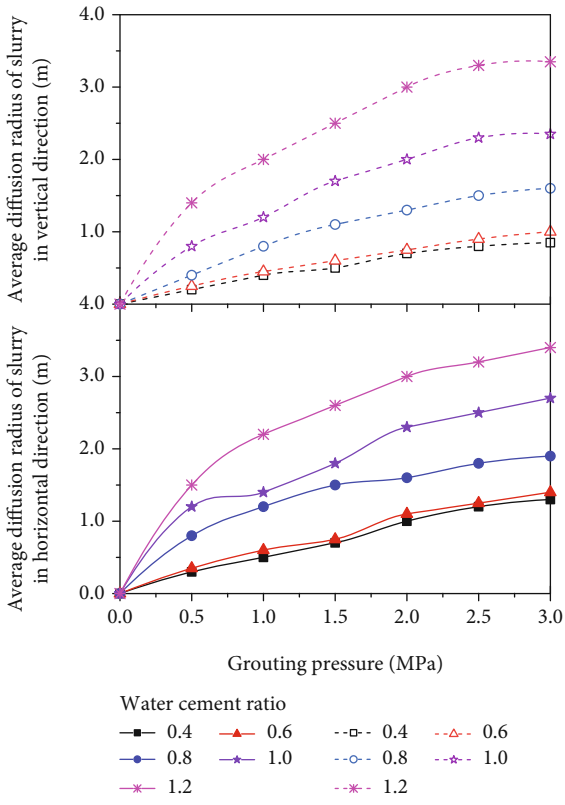

Figure 4: Variation law of slurry diffusion range.

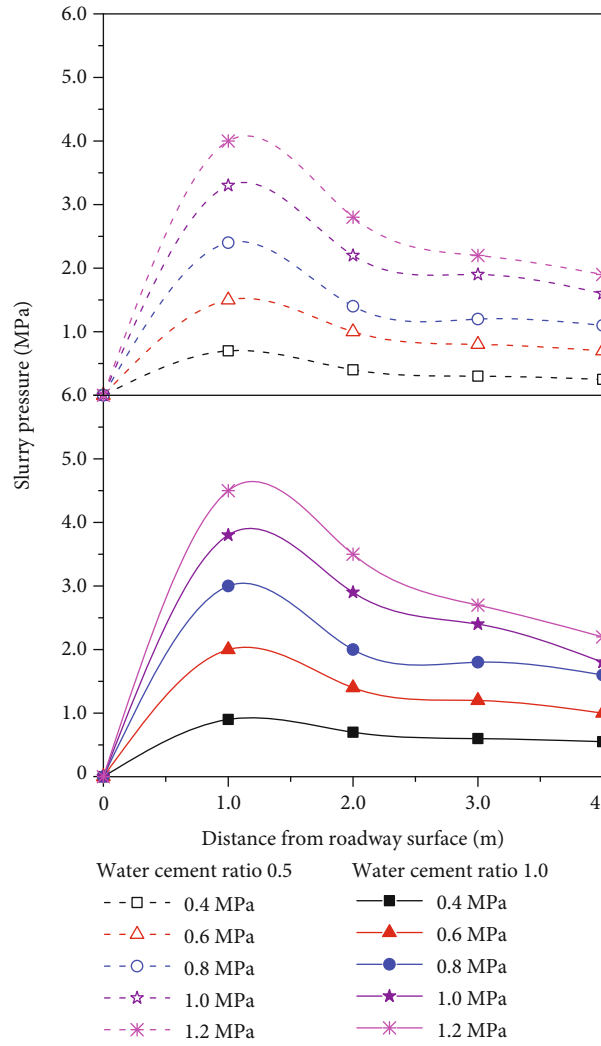

Figure 5: Grouting pressure distribution curve.

increase the stability of the structure, enhance the active support effect of anchor cable, and improve the control effect of surrounding rock.

3.5. Influence of Grouting on Surrounding Rock Displacement of Roadway. After roadway deformation and failure, the deformation of roadway under two different working conditions is shown in Figure 7. After bolt and cable support, the roadway roof subsidence is 260 mm, the displacement of two sides is 675 mm, and the floor heave is 208 mm; after bolt and cable support based on grouting, the roadway roof subsidence is 165 mm, the displacement of two sides is 432 mm, and the floor heave is 138 mm. The decline rates were 36.5%, 36%, and 33.7%, respectively. It can be seen from Figure 7 that under the two different working conditions, the deformation of roadway is relatively large, but after grouting reinforcement, the bearing capacity of surrounding rock of the roadway has limited improvement. The deformation of the roadway can be effectively controlled by implementing the reasonable support mode and parameters of bolt and cable.

3.6. The Influence of Grouting on the Supporting Structure. After the deformation and failure of the roadway, two different working conditions are used to repair and reinforce the roadway, and the stress situation of the roadway support structure is shown in Figure 8. It can be seen from Figure 8 that the loose range of the roadway is effectively controlled by grouting reinforcement of the broken roadway, and the cracks of loose circle are filled with slurry, so that the original broken surrounding rock is rereinforced, the shallow surrounding rock becomes relatively homogeneous, and the anchoring effect is improved. Compared with the simple bolt and cable support, the bolting structure with bolt and cable support based on grouting has better anchoring performance and more uniform stress. The anchorage structure of the roadway realizes balanced bearing, avoids the damage of support structure caused by local stress concentration, and increases the overall stability of the roadway.

4. Industrial Test

4.1. Engineering Background. The Qipanjing coal mine is located in Inner Mongolia, China, with a design production capacity of 0.3 Mt/a, a field area of 19.59 km^2, and a service life of 34.3 a. It adopts inclined shaft development, single level, and panel mining, and the main roadways are arranged along the 9# coal seam. The coal seam has a buried depth of 450 m, an average thickness of 2.91 m, and a complex structure with five layers of mudstone and gangue. The immediate roof is sandy mudstone (2.6 m), the main roof is coarse and fine sandstone (8.25 m), the immediate floor is sandy

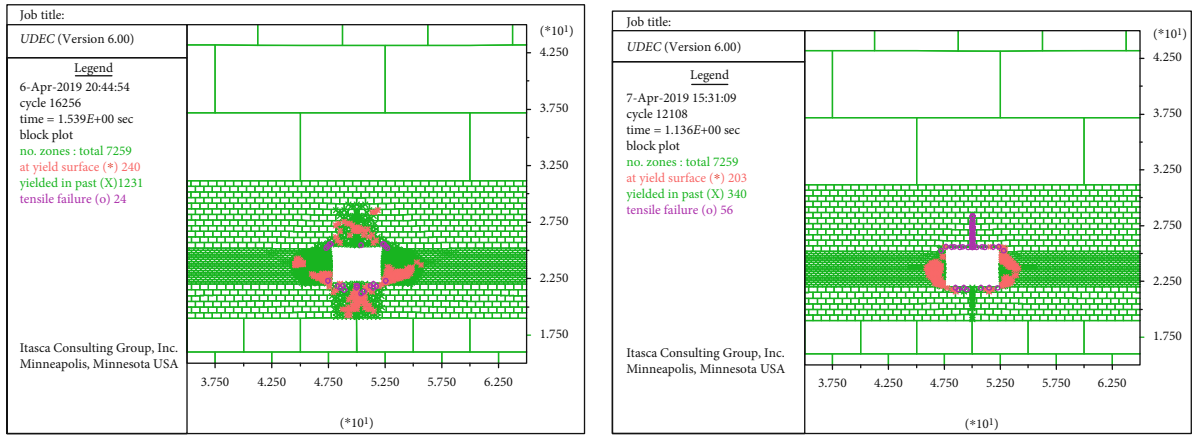

(a) Bolt and cable support (b) Grouting+bolt and cable support

Figure 6: Distribution characteristics of plastic zone in surrounding rock of roadway.

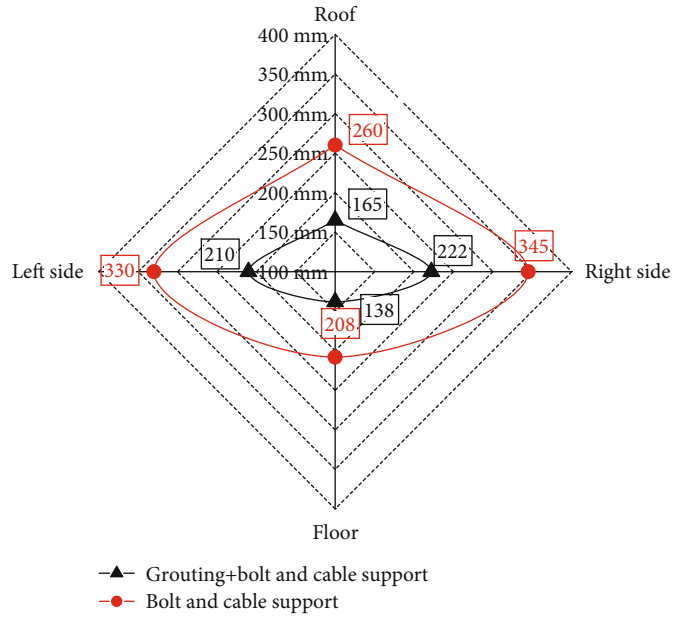

Figure 7: Deformation of surrounding rock of roadway.

mudstone (1.5 m), and the main floor is siltstone and sandy mudstone (5.05 m). Auxiliary transportation, belt transportation, and return air roadways (hereinafter referred to as roadway group) are arranged along the 9# coal seam roof. Due to the influence of mining on the two wings of the 020906 and 020907 working faces, the overall deformation is large and the damage occurs in different degrees. Among them, the auxiliary transportation roadway is the most serious, as shown in Figure 9.

4.2. Roadway Repair Principle. The roadway group has been disturbed by mining stress for many times. The loose circle of surrounding rock is large, the structure is loose and broken, the deformation of surrounding rock is large, and the local position is damaged and unstable. It is difficult to ensure the stability of the roadway with original bolt shotcrete support. Therefore, in order to ensure the normal operation of the mine, it is necessary to repair and reinforce the roadway group, restore the original design section, reshape the structure of the surrounding rock, improve the mechanical properties of the surrounding rock, and form a long-term effective support structure.

The grouting technology can fill the surrounding rock cracks, block the water passage, reduce the weathering and hydration of the surrounding rock, consolidate the surrounding rock into a whole, reduce the stress concentration coefficient of the surrounding rock, and provide a reliable anchoring foundation for the bolt and cable support. Meanwhile, the bolt and cable support system can form a certain supporting pressure on the surrounding rock after grouting

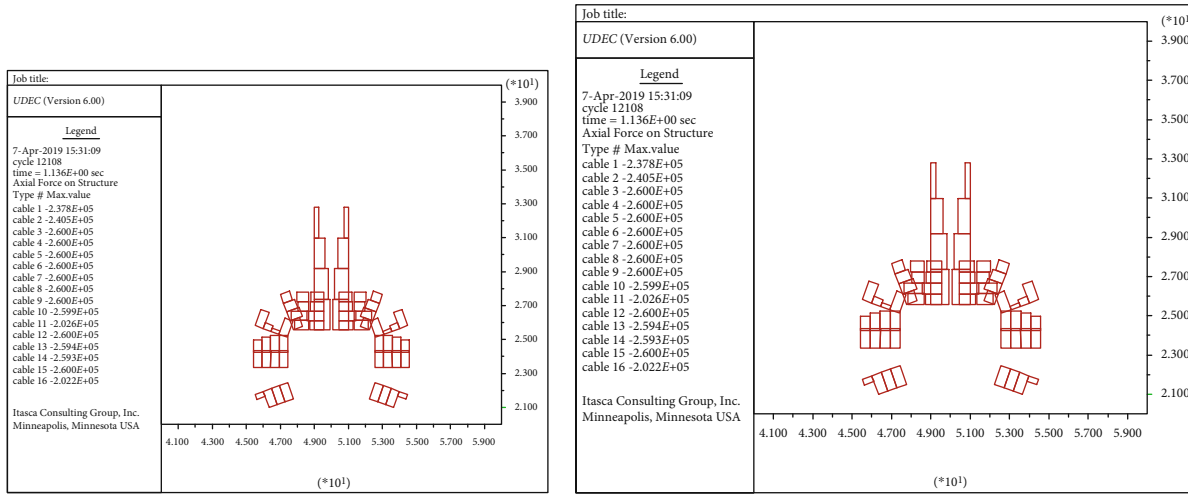

(a) Bolt and cable support

(b) Grouting+bolt and cable support

Figure 8: Stress state of roadway support structure.

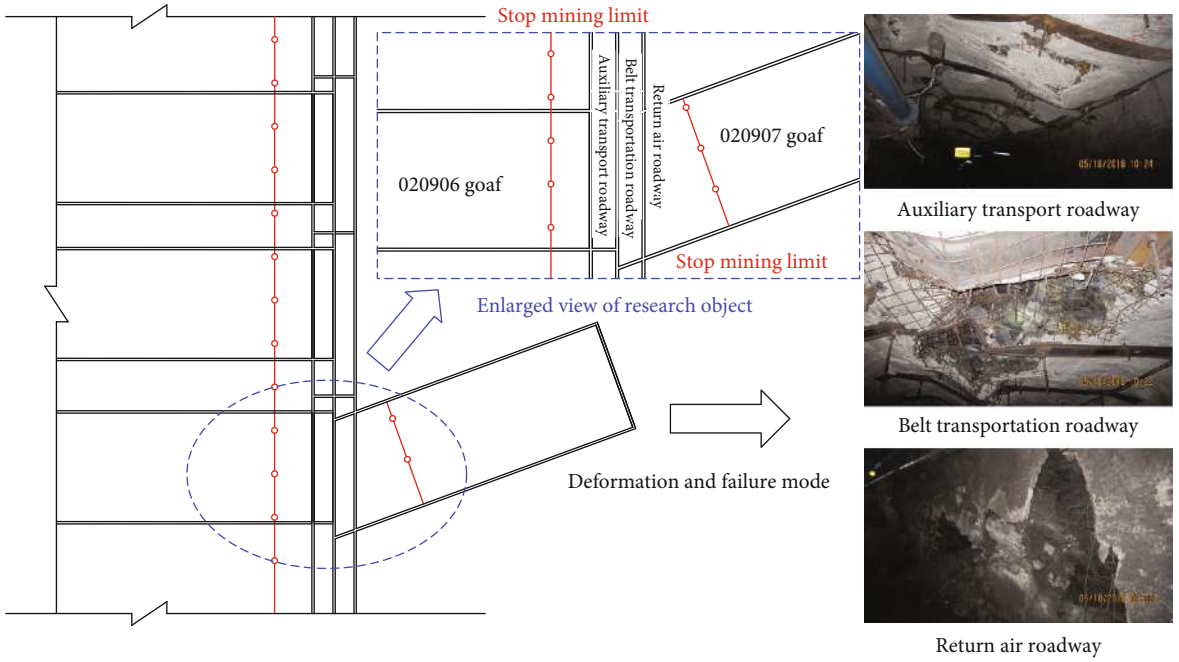

Figure 9: Roadway position and deformation and failure.

and improve the stress environment of the roadway. Therefore, the combination of the bolt, cable support, and grouting can help to form the reinforcement layer and reshape the structure of the surrounding rock.

4.3. Roadway Surrounding Rock Control Parameters

4.3.1. Grouting Parameters. The industrial test was carried out in the auxiliary transportation roadway. The grouting parameters of the roadway are shown in Table 9. The row spacing between grouting holes is mainly determined by the slurry diffusion radius, and the row spacing of the grouting holes is 0.6-0.8, twice the diffusion radius. Grouting is divided into two times: the first grouting hole is drilled according to the row spacing of 3.2 m, and the hole depth is 3.0 m; the second grouting hole is arranged in the middle of the first two rows of grouting holes, and the final row spacing is 1.6 m, as shown in Figure 10.

4.3.2. Bolt and Cable Support Parameters. According to the dynamic system design method, the roadway support parameters are obtained. Bolt parameters: HRB500, 20 mm in diameter, 2400 mm in length, and 80 mm in yield distance are used in the roof and sides, with the spacing of 800 mm × 800 mm; the 10# wire mesh is laid and the diameter of 14 mm steel ladder beam is connected. Cable parameters: the roof is supported by high-strength prestressed yield cable with a diameter of 21.6 mm, length of 8300 mm, and yield distance of 120 mm, with spacing of 2000 mm × 2400 mm;

Table 9: The grouting parameters.

Serial number	Project	Parameters
1	Grouting materials	Modified grouting material
2	Water cement ratio	1.5 : 1
3	Lag grouting time	3-5 days after shotcreting
4	Grouting pipe	R25N self-drilling grouting anchor with length of 2.5 m and yield strength of 150 kN
5	Grouting pressure	2.0-3.0 MPa
6	Grouting quantity	Stop grouting when the design grouting pressure is reached or a large amount of grout leakage occurs
7	Slurry diffusion radius	About 2.5 m
8	Depth of grouting hole	3.0 m

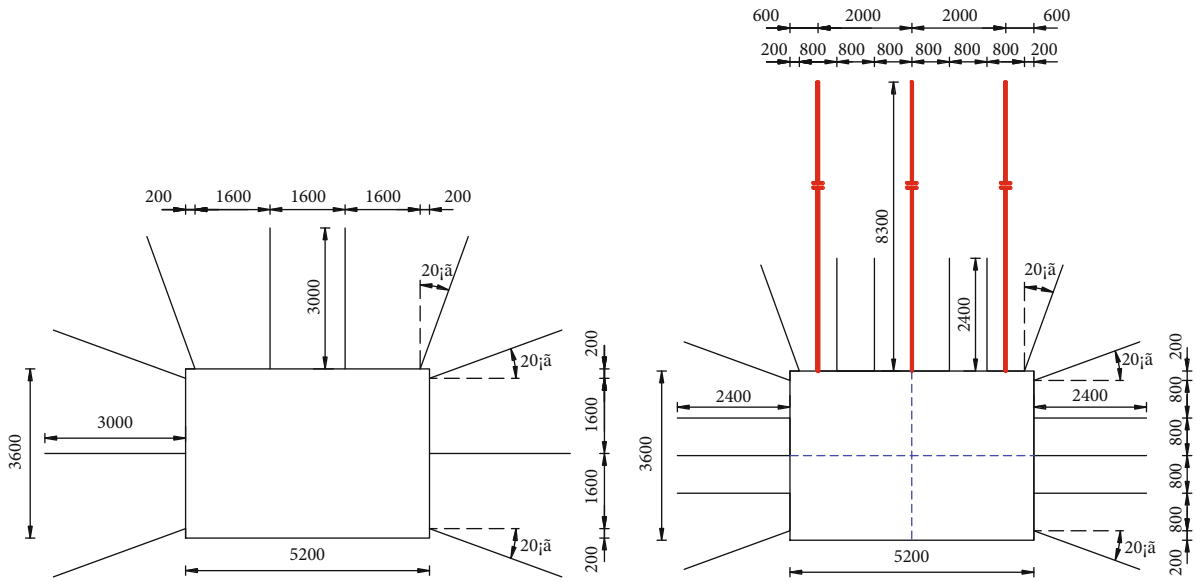

(a) Grouting section

(b) Support section

Figure 10: Roadway section with repair and reinforcement.

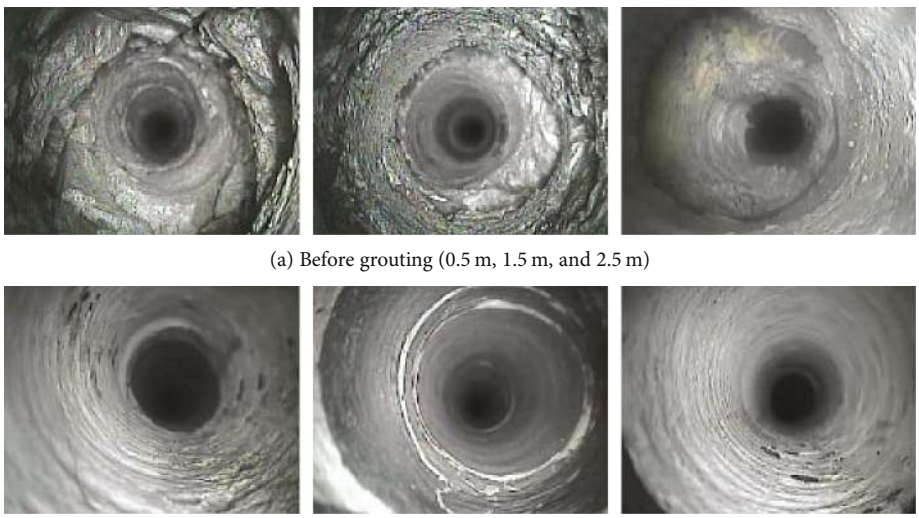

(a) Before grouting (0.5 m, 1.5 m, and 2.5 m)

(b) After grouting (0.5 m, 1.5 m, and 2.5 m)

Figure 11: Borehole peep.

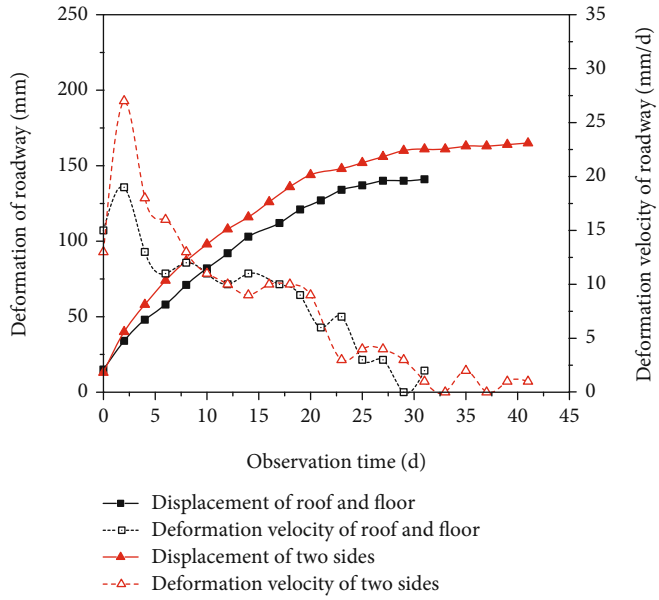

Figure 12: Surface displacement curve.

M-shaped steel strip with thickness of 3.5 mm is connected, as shown in Figure 10.

4.4. Mine Pressure Monitoring and Analysis. After the reinforcement and repair of auxiliary transportation roadway, two stations were set up at an interval of 20 m to monitor the grouting effect and surface displacement.

4.4.1. Borehole Peeping. YTJ20 rock detector is used to carry out borehole detection, as shown in Figure 11. Before grouting, the shallow part of the roof is completely broken, there are a lot of cracks, and the integrity is poor; after grouting, the broken coal and rock mass is fully cemented and evenly distributed, and the surrounding rock strength is strengthened. The grouting effect of the two sides is similar.

4.4.2. Surface Displacement. After the roadway is repaired and reinforced, the stability period of the surrounding rock is about 25 days. Due to grouting and high-strength yielding bolt and cable reinforcement support from the reinforcement layer, the bearing capacity of surrounding rock is significantly improved, the surrounding rock deformation is uniform, and the overall deformation is small, and the section meets the production requirements, as shown in Figure 12.

5. Conclusions

(1) Based on the defects of existing grouting materials and the characteristics of a coal mine roadway, a modified grouting material was developed by using the double liquid grouting mode. The material is composed of two groups of dry materials A and B, which are mixed with water and in equal amounts. The material A is made of Portland cement and material B is made of sulphoaluminate cement. The influence of component content on the physical and mechanical properties of grouting materials was studied by orthogonal test, and the optimal ratio was obtained, in which the water-cement ratio was 0.8 : 1 and the mass ratio of cement, fly ash, bentonite, and water was 1 : 0.3 : 0.1 : 1.44. Considering from the perspective of improving the compressive strength of the slurry stone, the optimized ratio of admixture content is selected, and the mass ratio of water reducing agent C : accelerator D : retarder E is 1.5% : 0.05% : 0.3%

(2) By means of numerical simulation, the influence of grouting parameters and grouting pressure of modified grouting material on grouting flow properties is simulated. The reinforcement effect of modified grouting material on surrounding rock properties of the roadway is mainly studied, and the rules of modified grouting material on surrounding rock properties of roadway are revealed: grouting makes the surrounding rock stress transfer from deep to shallow, and the surrounding rock stress distribution is more uniform. Broken surrounding rock grouting can improve the mechanical properties of roadway surrounding rock, enhance the stability of roadway surrounding rock, control the deformation of roadway surrounding rock, and realize the balanced bearing of roadway surrounding rock anchorage structure. The feasibility of the application of modified grouting material in tunnel grouting engineering is verified

(3) The results obtained by theoretical analysis, laboratory test, and numerical simulation are applied to the practice of roadway repair and reinforcement of the north roadway group in the Qipanjing coal mine.

The field monitoring data show that the production practice was well guided with the repair and reinforcement technology with high-strength yielding bolt and shallow grouting reinforcement as the core, and the modified grouting material has good effect on grouting reinforcement of roadway surrounding rock

Data Availability

The data in the manuscript can be available on request through Dingchao Chen, whose email address is chendingchaoxzit@163.com.

Conflicts of Interest

The authors declare that they have no known competing financial interests or personal relationships that could have appeared to influence the work reported in this paper.

Acknowledgments

This work was supported by the National Natural Science Foundation of China (grant numbers 51904296, 52074240, and 51974296), the Outstanding Backbone Teachers of "Innovation Project" of the University in Jiangsu Province, China, in 2020, and Major Projects of Natural Science Foundation of Universities in Jiangsu Province, China (grant number 20KJA560001). The sources of this support are gratefully acknowledged.

References

[1] H. P. Kang, G. Xu, B. M. Wang et al., "Forty years development and prospects of underground coal mining and strata control technologies in China," *Journal of Mining and Strata Control Engineering*, vol. 1, no. 1, article 013501, 2019.

[2] G. Wang, F. Liu, Y. Pang, H. Ren, and Y. Ma, "Coal mine intellectualization: the core technology of high quality development," *Journal of China Coal Society*, vol. 44, no. 2, pp. 349–357, 2019.

[3] M. He, Z. Ma, Z. Guo, and S. Chen, "Key parameters of the gob-side entry retaining formed by roof cutting and pressure release in deep medium-thickness coal seams," *Journal of China University of Mining and Technology*, vol. 47, no. 3, pp. 468–477, 2018.

[4] M. Qian and J. Xu, "Behaviors of strata movement in coal mining," *Journal of China Coal Society*, vol. 44, no. 4, pp. 973–984, 2019.

[5] C. Hou, "Key technologies for surrounding rock control in deep roadway," *Journal of China University of Mining and Technology*, vol. 46, no. 5, pp. 970–978, 2017.

[6] J. X. Zhang, Q. Zhang, F. Ju, N. Zhou, M. Li, and Q. Sun, "Theory and technique of greening mining integrating mining, separating and backfilling in deep coal resources," *Journal of China Coal Society*, vol. 43, no. 2, pp. 377–389, 2018.

[7] N. Zhang, X. Xue, and F. Han, "Technical challenges and countermeasures of the co-excavation of coal and gas with no-pillar retains in deep coalmine," *Journal of China Coal Society*, vol. 40, no. 10, pp. 2251–2259, 2015.

[8] W. Wang, C. Yuan, W. J. Yu et al., "Stability control method of surrounding rock in deep roadway with large deformation," *Journal of China Coal Society*, vol. 41, no. 12, pp. 2921–2931, 2016.

[9] X. Q. Qi, Y. S. Pan, H. T. Li et al., "Theoretical basis and key technology of prevention and control of coal-rock dynamic disasters in deep coal mining," *Journal of China Coal Society*, vol. 45, no. 5, pp. 1567–1584, 2016.

[10] Y. Wu, D. Yun, P. Xie, Z. D. Fan, D. F. Wang, and Y. H. Zhang, "Progress, practice and scientific issues in steeply dipping coal seams fully-mechanized mining," *Journal of China Coal Society*, vol. 45, no. 1, pp. 24–34, 2020.

[11] M. He, Y. Gao, J. Yang, and W. Gong, "An innovative approach for gob-side entry retaining in thick coal seam longwall mining," *Energies*, vol. 10, no. 11, p. 1785, 2017.

[12] Y. Wu, F. Gao, J. Chen, and J. He, "Experimental study on the performance of rock bolts in coal burst-prone mines," *Rock Mechanics & Rock Engineering*, vol. 52, no. 10, article 1794, pp. 3959–3970, 2019.

[13] L. Yuan, "Research progress on risk identification, assessment, monitoring and early warning technologies of typical dynamic hazards in coal mines," *Journal of China Coal Society*, vol. 45, no. 5, pp. 1557–1566, 2019.

[14] S. Q. Yang, M. Chen, H. W. Jing, K. F. Chen, and B. Meng, "A case study on large deformation failure mechanism of deep soft rock roadway in Xin'An coal mine, China," *Engineering Geology*, vol. 217, pp. 89–101, 2017.

[15] H. Kang, X. Zhang, L. Si, F. Gao, and Y. Wu, "In-situ stress measurements and stress distribution characteristics in underground coal mines in China," *Engineering Geology*, vol. 116, no. 3-4, pp. 333–345, 2010.

[16] J. Zhang and Y. Sun, "Experimental and mechanism study of a polymer foaming grouting material for reinforcing broken coal mass," *KSCE Journal of Civil Engineering*, vol. 23, no. 1, pp. 346–355, 2019.

[17] X. Gao, X. Wang, and X. Liu, "New chemical grouting materials and rapid construction technology for inclined shaft penetrating drift-sand layer in coal mine," *Advances in Materials Science and Engineering*, vol. 2018, Article ID 2797419, 5 pages, 2018.

[18] C. Liu, J. Yang, and F. Wu, "A proposed method of coal pillar design, goaf filling, and grouting of steeply inclined coal seams under water-filled strata," *Mine Water and the Environment*, vol. 34, no. 1, pp. 87–94, 2015.

[19] R. Pan, Q. Wang, B. Jiang et al., "Failure of bolt support and experimental study on the parameters of bolt- grouting for supporting the roadways in deep coal seam," *Engineering Failure Analysis*, vol. 80, pp. 218–233, 2017.

[20] D. Xuan, B. Wang, and J. Xu, "A shared borehole approach for coal-bed methane drainage and ground stabilization with grouting," *International Journal of Rock Mechanics & Mining Sciences*, vol. 86, pp. 235–244, 2016.

[21] X. Ao, X. Wang, X. Zhu, Z. Zhou, and X. Zhang, "Grouting simulation and stability analysis of coal mine goaf considering hydromechanical coupling," *Journal of Computing in Civil Engineering*, vol. 31, no. 3, article 04016069, 2017.

[22] Y. Sun, G. Li, J. Zhang, and D. Qian, "Stability control for the rheological roadway by a novel high-efficiency jet grouting technique in deep underground coal mines," *Sustainability*, vol. 11, no. 22, article 6494, 2019.

[23] X. Sun, L. Wang, Y. Lu, B. Jiang, Z. Li, and J. Zhang, "A yielding bolt-grouting support design for a soft-rock roadway

under high stress: a case study of the Yuandian no. 2 coal mine in China," *Journal of the Southern African Institute of Mining and Metallurgy*, vol. 118, no. 1, pp. 71–82, 2018.

[24] T. Zhao and C. Liu, "Roof instability characteristics and pre-grouting of the roof caving zone in residual coal mining," *Journal of Geophysics and Engineering*, vol. 14, no. 6, pp. 1463–1474, 2017.

[25] G. Lu, Y. Wang, Y. Zhang, and S. T. Ariaratnam, "Feasibility of using sodium silicate as grouting in loose coal bed sections for methane drainage," *Tunnelling & Underground Space Technology*, vol. 72, pp. 107–113, 2018.

[26] K. T. Crane and T. R. West, "Prioritizing grouting operations for abandoned underground coal mines, southwestern Indiana," *Asian Journal of Chemistry*, vol. 26, no. 5, pp. 1509–1512, 2014.

[27] J. Xia, Q. Su, and D. Liu, "Optimal gypsum-lime content of high water material," *Materials Letters*, vol. 215, pp. 284–287, 2018.

[28] X. Zhou, C. Liu, Y. Liu, C. Wang, and Y. J. Ma, "Effect of dry-wet cycling on the mechanical properties of high-water materials," *Advances in Civil Engineering*, vol. 2020, Article ID 2605751, 11 pages, 2020.

[29] L. Calvo and J. Casas, "Sterilization of biological weapons in technical clothing and sensitive material by high-pressure CO_2 and water," *Industrial & Engineering Chemistry Research*, vol. 57, no. 13, pp. 4680–4687, 2018.

[30] G. Hu, W. He, and C. Lan, "Sealing behavior and flow mechanism of expandable material slurry with high water content for sealing gas drainage boreholes," *Geofluids*, vol. 2018, Article ID 2954306, 15 pages, 2018.

[31] Y. Zhang, Y. Wang, T. Li, Y. Sun, and Z. Xiong, "Effects of lithium carbonate on performances of sulphoaluminate cement-based dual liquid high water material and its mechanisms," *Construction & Building Materials*, vol. 161, pp. 374–380, 2018.

[32] J. Lee and T. Lee, "Effects of high CaO fly ash and sulfate activator as a finer binder for cementless grouting material," *Materials*, vol. 12, no. 22, 2019.

[33] J. Lee, G. Kim, Y. Kim, K. Mun, and J. Nam, "Engineering properties and optimal conditions of cementless grouting materials," *Materials*, vol. 12, no. 19, 2019.

[34] H. Shimada, A. Hamanaka, T. Sasaoka, and K. Matsui, "Behaviour of grouting material used for floor reinforcement in underground mines," *International Journal of Mining, Reclamation and Environment*, vol. 28, no. 2, pp. 133–148, 2014.

[35] Y. Yu, J. Bai, X. Wang, and L. Zhang, "Control of the surrounding rock of a goaf-side entry driving heading mining face," *Sustainability*, vol. 12, no. 7, article 2623, 2020.

[36] H. Li, Y. Zhang, L. Xu, X. Jia, and X. Gu, "Examination of the treatment quality of filling mined-out voids using super-high-water material by the TEM technique," *Environmental Earth Sciences*, vol. 76, no. 3, article 6431, 2017.

[37] J. Kim, G. Yoon, H. Kim, K. Kang, and Y. U. Park, "$Na_3V(PO_4)_2$: a new layered-type cathode material with high water stability and power capability for Na-ion batteries," *Chemistry of Materials*, vol. 30, no. 11, pp. 3683–3689, 2018.

[38] Y. Yu, X. Wang, J. Bai, L. Zhang, and H. Xia, "Deformation mechanism and stability control of roadway surrounding rock with compound roof: research and applications," *Energies*, vol. 13, no. 6, article 1350, 2020.